

Beamforming Techniques Performance Evaluation for 5G massive MIMO Systems

Irina Stepanets¹, Grigoriy Fokin², Andreas Müller³

¹ Deutsche Telekom, Technische Planung und Rollout, Landgrabenweg 151,
53227 Bonn, Germany

irina.stepanets@telekom.de

² The State University of Telecommunication St. Petersburg, Prospect Bolshevnikov 22,
193232 St. Petersburg, Russia Federation

grihafokin@gmail.com

³ Hochschule Darmstadt, Haardtring 100,
64295 Darmstadt, Germany

andreas.mueller@h-da.de

Abstract. The estimation of the direction of arrival (DOA) and beamforming are the effective methods for the realization of spatial diversity. Several approved algorithms already exist for DOA and beamforming. The purpose of this work is to verify the application of these existing algorithms for the massive multiple-input multiple-output (massive MIMO) antenna systems in the fifth generation wireless communication (5G). This investigation provides simulation results of adaptive beamforming techniques with various planar array configurations for massive MIMO and analyzes accuracy of the adaptive massive MIMO antenna diagram according to the 5G requirements. Results of the current research revealed that with the growth of the antenna elements from 128 not only the accuracy of the beamforming increases up to 4° resolution, but also null steering becomes precise, which provides interference suppression up to 340 dB and accordingly meets 5G requirements up to 5° precision.

Keywords: 5G, massive MIMO, DOA, adaptive beamforming, LMS, planar array, accuracy of beamforming, null steering.

1 Introduction

The development of the next generation wireless communication 5G demands much higher requirements in comparison to the previous mobile generation. According to the last technical specification, 5G technology should guarantee a higher capacity up to 7,5 Tbps/km², higher data rate up to 1 Gbps in DL and 500 Mbps in uplink (UL) [1] and accordingly substantially higher requirements for angular resolution in down-

link (DL) [1, 2]. 3GPP defines following angular resolution requirement: for moving UE with speed up to 0,5 m/s it is defined to be less than 5° , for the moving UE with speed up to 10 km/h it is defined to be less 10° and for the static UE it is defined be less than 30° [1]. To realize these requirements in 4th generation networks (4G) is impossible, so for 5G completely new technological solutions are needed. The massive MIMO technology in turn implies a large amount of antenna elements in arrays, which is a precondition for a successful DOA and beamforming applications. That's why the massive MIMO with its DOA and beamforming capabilities is one of the most promising technology, which can meet defined 3GPP requirements for 5G.

The combination of both techniques, DOA and beamforming, enables robust and spectrally efficient communication in a desired destination to a UE. DOA is a signal processing technique, which estimates the bearing of the source location of corresponding incoming signal. While an adaptive beamforming is a technique to form and to steer a maximum radiation pattern of antenna into the bearing direction of interest, whereas radiation pattern null are placed into the bearing direction of interfering sources [3, 4, 5]. In particular, in 5G network particular interest lies in the steering of the main lobe of the antenna, mounted on the Next Generation Node Base (gNB), to a special user equipment (UE) location [6].

Two techniques, DOA and beamforming, are associated with each other: firstly, it is necessary to estimate correctly a DOA of UE in order to set a corresponding direction of a beam from a gNB antenna, and secondly, to steer cooperatively a maximum radiation of antenna in the bearing direction of UE. This cooperation admits to carry out a reliable transmission between gNB and UE with high signal-to-noise ratio (SNR) and low interference impact.

The material in the paper is organized in the following order. DOA and Beamforming Techniques are formalized in Section 2. Simulation scenario and results are given in Section 3. Finally, we draw the conclusions in Section 4.

2 DOA and Beamforming Techniques

2.1 DOA Preliminaries

The initial condition of high precision beam steering is correct DOA availability. The estimation of the DOA is based on the measurements of time delays of incoming wave front to the different antenna elements. Desired signal for DOA is termed as signal-of-interest (SOI), whereby the interfering signal is termed as signal-not-of-interest (SNOI). There are different methods of DOA estimation [7]. The most popular of them are Capon's method, MULTiple SIGNAL Classification (MUSIC) algorithm and the Estimation of Signal Parameters via Rotational Invariance Technique (ESPRIT) [3].

In this work we assume that DOA was correctly estimated beforehand, that is why we further consider mathematical preliminaries of beamforming techniques.

2.2 Beamforming techniques

The purpose of the beamforming is to generate a beam of a necessary shape and to direct it to a desired location in real time, while suppressing interference [8, 9]. To fulfill this, the signal processing on the gNB requires advanced beamforming capabilities [8]. There are various methods to accomplish beamforming, which are discussed in the further classification due to the different categories.

In [3] beamforming classification includes two realizations: *switched-beam* and *adaptive array*.

Switched-beam system realization utilizes predefined number of lobes in a beam-pattern and switches between them during connection. There are several switched beamforming techniques such as Butler matrix [10], Blass matrix [11], or Wullenweber array [12].

In adaptive array systems there are no predefined beams, but the antenna diagram changes its shape and direction toward each dedicated UE adaptively, providing more degrees of freedom. These technique is based on the so called *weighting* approach. This means that the complex weights w_i are instantaneously calculated by an adaptive algorithm (fig. 1), in order to direct the maximum antenna radiation pattern toward the UE and to steer null toward interference sources. In this sense the adaptive beamforming is an iterative approximation of an optimal beamforming [13].

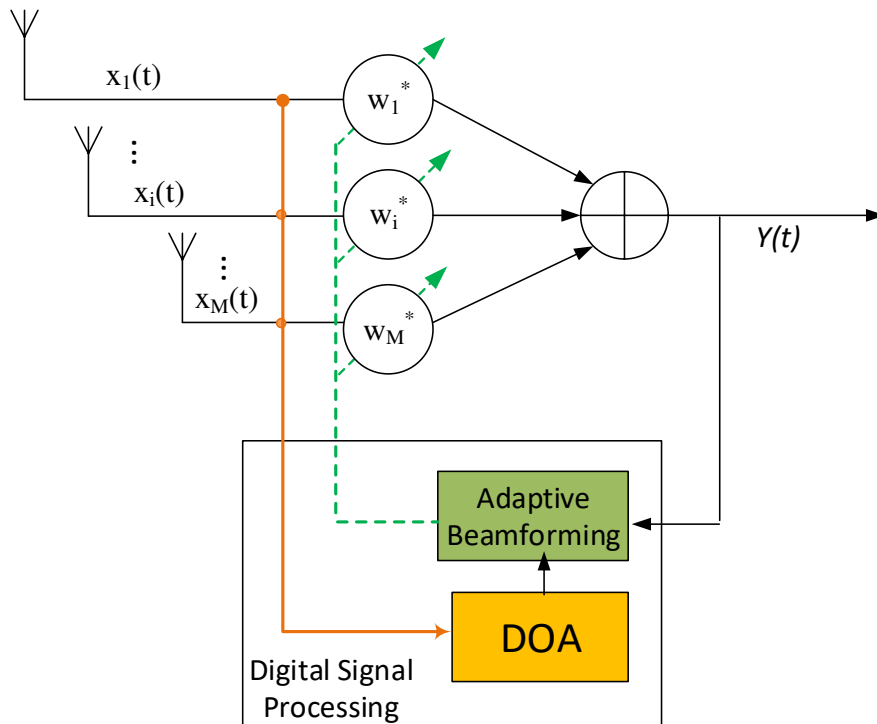


Fig. 1. Block diagram of DOA and adaptive beamforming cooperation [3]

The weights w_i can be generally described by [14]

$$w_i = p_i e^{j\varphi_i}, \tag{1}$$

where p_i is a gain magnitude and φ_i is a phase shift of i^{th} RF antenna element.

Output signal, multiplied by the beamforming weights on the receiving site, can be represented by [15]

$$y = \sum_{i=1}^K w_i^* x_i = \mathbf{w}^H \mathbf{x}, \quad (2)$$

where y is an output signal after receiving adaptive beamformer, x_i is a signal arriving from angle φ_i , \mathbf{w} represents the K -length vector of weights, \mathbf{x} represents the K -length vector of received signals and the superscript H is the Hermitian operator (conjugate transpose). Expressions (1) and (2) include calculations to emphasize signals from a dedicated direction while attenuating those from the non-of-interest directions, which can interfere with the useful signal. This process is called as adaptive beamforming. In this work the adaptive beamforming is the subject of investigation as the most attractive technology for the 5G wireless communications [16, 17, 18].

Various algorithms for the adaptive beamforming exist, while most widely implemented of them are Least Mean Square (LMS), Normalized Least Mean Square (NLMS), Recursive Least Square (RLS), Sample Matrix Inversion (SMI), and Hybrid Least Mean Square / Sample Matrix Inversion (LMS/SMI) [3, 19]. In current work and further simulations LMS algorithm is implemented as it is considered to have least computational complexity and high convergence stability [3, 20].

The functionality of the LMS algorithms is represented as follows. The output of the antenna array can be expressed as $y(t)$ (3) [20]:

$$y(t) = s(t)a(\theta_0) + \sum_{i=1}^{N_u} u_i(t)a(\theta_i) + n(t), \quad (3)$$

where $s(t)$ denotes the desired signal arriving at angle θ_0 and $u_i(t)$ denotes interfering signals arriving at angle θ_i ; $a(\theta_0)$ and $a(\theta_i)$ represent the steering vectors for the desired and interfering signals respectively; $n(t)$ is additive noise.

According to the optimization theory approach, named gradient method of steepest decent, the definition of weights can be done by

$$w(n+1) = w(n) - \mu \nabla(E\{e^2(n)\}), \quad (4)$$

where $w(n+1)$ is an updated weight, $w(n)$ is a previous weight, μ is a step size and controls the convergence characteristics of LMS, E depicts an expected value of the mean square error $e^2(n)$, which can be described by

$$e^2(n) = [d - y]^2, \quad (5)$$

where one can observe that the $e^2(n)$ is mean square error between the beamformer output y and the reference signal d .

The gradient represents a vector of partial derivations of mean square error E with respect to weights:

$$\nabla(E\{e^2(n)\}) = \begin{bmatrix} \frac{\partial(E\{e^2(n)\})}{\partial w_0} \\ \vdots \\ \frac{\partial(E\{e^2(n)\})}{\partial w_L} \end{bmatrix}. \quad (5)$$

Using this LMS method, the following simulations were done in order to steer beam toward the desired signal and to place null toward the interfering one.

Another category for the beamforming classification can be defined according to the placement of digital-to-analog converter (DAC). If single DAC is used for all of antenna elements, *analog beamforming* term is used. In contrast to this, if multiple DACs are implemented after each antenna element and the processing of signals from all antenna elements is done simultaneously, then *digital beamforming* term is used. Both schemes have pros and cons.

Analog beamforming scheme has a lower power consumption and lower computation complexity than a digital one. From the other hand as only a single radio-frequency (RF) chain for all antenna elements in the analog scheme is available, it is possible to form a beam only to a single direction at any given time [6]. Whereby the digital scheme has more flexibility and allows to form a beam in many directions simultaneously. However, digital scheme requires a dedicated RF chain for each antenna element, which increases a transmit power.

To improve the power consumption parameters and still to benefit from the multiple directional beamforming at the same time the *hybrid* beamforming technique was developed. It combines the advantages from the former both and is recommended for 5G applications by 3GPP [21]. The DACs are coupled via RF chains (fig. 2) with the specified groups of antenna elements, but not with each of them, which reduces the power consumption and provides a sufficient number of analog beams into the different directions at the same time [6].

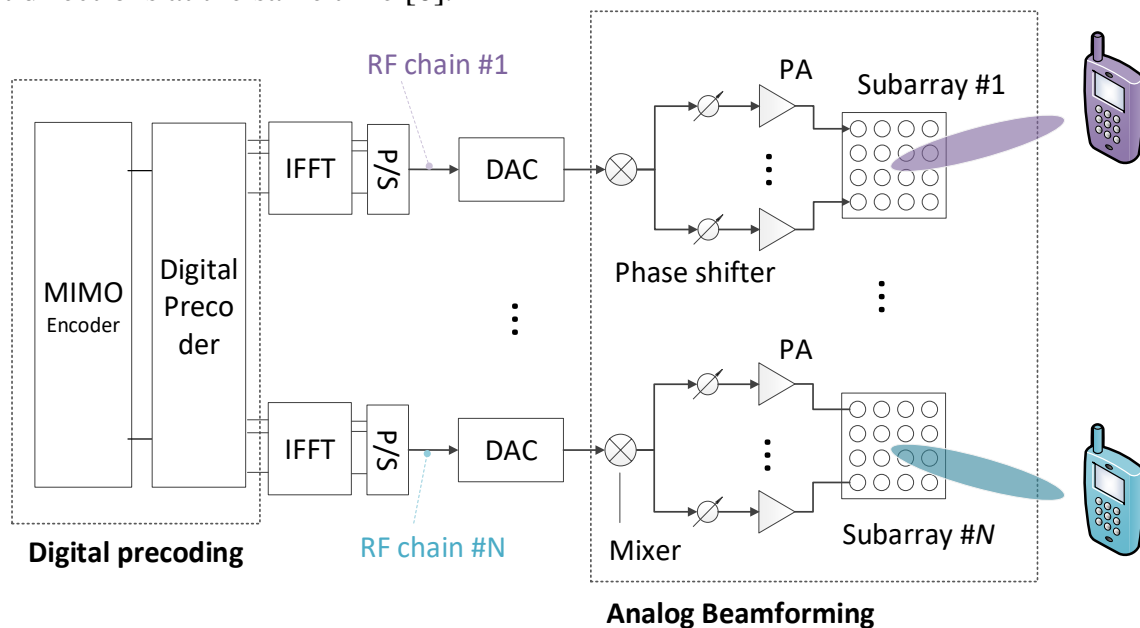


Fig. 2. Block diagram of hybrid beamformer [21]

The next one category in the beamforming classification is antenna elements configuration. Antenna elements can be arranged in various geometries, for example, in linear, circular or planar configurations [7]. In this work planar antenna array is investigated and simulated as it is recommended by 3GPP for 5G, where it is termed as uniform rectangular panel array (URPA) [22].

In the next section we will describe simulation scenario to illustrate our investigation.

3 Simulation Results

3.1 Simulation scenario

Given initial conditions in these simulations were chosen regarding to the 3GPP requirements for the angular resolution up to 5° in 5G wireless communications, as described in section 1. Namely the assumption for the simulation was made as follows (fig. 3), the UE with SOI is located with the elevation angle $\theta=32^\circ$ and azimuth angle $\varphi=50^\circ$ related to the gNB; the interfering UE with SNOI is located close to the SOI UE with $\theta=36^\circ$ and $\varphi=54^\circ$, and results in only 4° deference between the SOI UE and SNOI UE in both elevation and azimuth direction. Therefore, this scenario assumption satisfies 3GPP requirement with 1° margin.

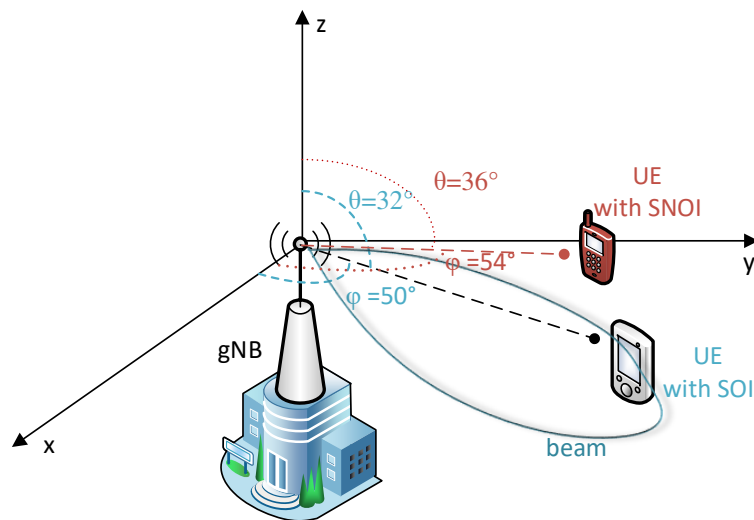


Fig. 3. Assumption of the UE positioning for beamforming simulations

The gNB antenna system is placed in the point of origin of the coordinate system. Fixing these positioning parameters for UEs and gNB, different antenna array configurations on gNB were investigated in order to investigate which configuration is appropriate to attain the beamforming accuracy in 5G requirements.

Another assumption in this simulation is that the DOA were estimated correctly and thereby known in advance.

As justified previously in this work, the adaptive beamforming with LMS algorithm and the antenna system on gNB with planar array were considered to be used for the simulation. The planar array was investigated with various number of antenna elements. As actual developments of massive MIMO systems are focused currently on antenna arrays with 64 and 128 antenna ports, in this work these antenna elements

number are taken as a foothold for the further investigations. To analyze the lower and upper boundaries, the planar arrays with 16, 256 and 1024 antennas elements were taken into the account. The sequence of simulation cases is considered as follows. The first scenario includes $4 \times 4 = 16$ antenna elements in a planar array; the second scenario $8 \times 8 = 64$ antenna elements; the third scenario $8 \times 16 = 128$ antenna elements; the fourth scenario $16 \times 16 = 256$ antenna elements and the fifth scenario includes $32 \times 32 = 1024$ antenna elements.

The goal of the simulation is to investigate, how precise is LMS beamforming and null steering technique realization for the scenario including UE with SOI and UE with SNOI, depending on the different antenna elements number.

3.2 Simulation results

The simulation results of the assigned task are illustrated in the fig. 4-8 and described further.

In the fig. 4. the beamforming pattern of planar array with 16 elements is presented.

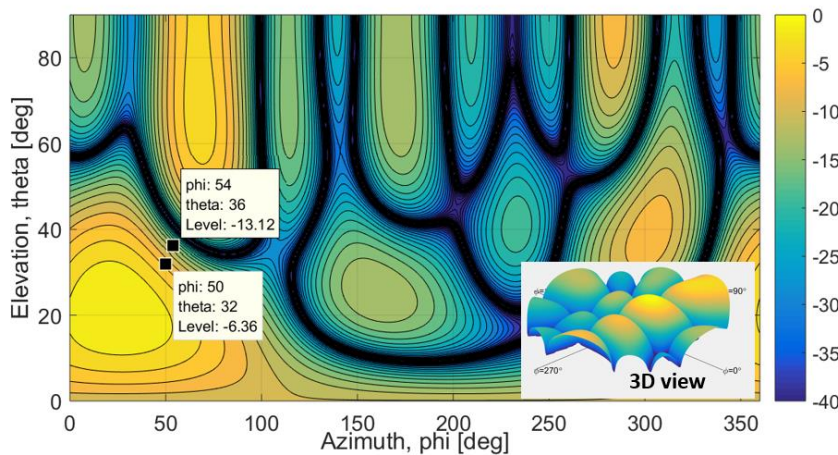


Fig. 4. Adaptive beamforming pattern using planar array with $4 \times 4 = 16$ elements, SOI: $\theta = 32^\circ$, $\varphi = 50^\circ$; SNOI: $\theta = 36^\circ$, $\varphi = 54^\circ$

The maximum radiation of antenna is depicted as a bright yellow area and in this case is directed quite close to the desired location of SOI UE ($\theta = 32^\circ$, $\varphi = 50^\circ$). However, this maximum does not achieve the SOI UE, but SOI UE lays still in the slope of maximum (depicted as orange area) with the radiation level by $-6,36$ dB. The interfering source, UE SNOI, lays in the position of elevation $\theta = 36^\circ$ and azimuth $\varphi = 54^\circ$. So the radiation from gNB antenna is supposed to be suppressed in this direction by null steering (minimum of radiation is colored in black on the diagram). However, the radiation field in this location, at $\theta = 36^\circ$ and $\varphi = 54^\circ$, is $-13,12$ dB, which does not correspond to the null of the antenna pattern, but lays in the piedmont of the beam and marked in green color. So, the difference in the beam radiation level between the desired UE and interfering UE is $6,76$ dB. For the better visuality the 3D view of the pattern is placed in the right corner of the figure, whereby the color palette replicates

2D layout, bright yellow means the highest value of the field strength, colors from dark blue till the black means the lowest value of the radiation field strength.

The next simulation case uses the same position coordinates SOI UE ($\theta=32^\circ$, $\varphi=50^\circ$) and SNOI UE ($\theta=36^\circ$, $\varphi=54^\circ$), but applies a planar array with $8 \times 8 = 64$ antenna elements. The results of the the second simulation case are depicted in the fig. 5. One can observe on this diagram, that the maximum of the beam became more concentrated on the one spot and the beam pattern grew narrow in comparison to the first simulation case. Herewith at the location of SOI UE the value of the radiation field strength is $-5,076$ dB and at the SNOI UE location $-133,2$ dB, which provides a much better diversity of about 128 dB suppression between two terminals, than in the first case. This practically exludes the interference impact.

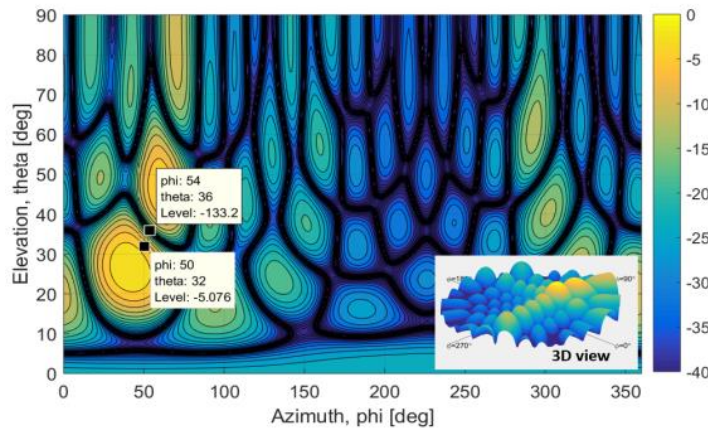


Fig. 5. Adaptive beamforming pattern using planar array with $8 \times 8 = 64$ elements, SOI: $\theta = 32^\circ$, $\varphi = 50^\circ$; SNOI: $\theta = 36^\circ$, $\varphi = 54^\circ$

The third simulation case with its 128 antenna elements represents an interest in the actual developments in massive MIMO systems. The results of this simulation are depicted in fig. 6. The radiation concentration got much more focused on the spot of interest and the beam became even more narrower than at the second case. To SOI UE is dedicated higher radiation level $-1,087$ dB and one can see in the diagram that the SOI UE is now inside of the bright yellow ring. From the other side the null is placed exactly on the SNOI UE spot with its radiation field strength $-333,4$ dB.

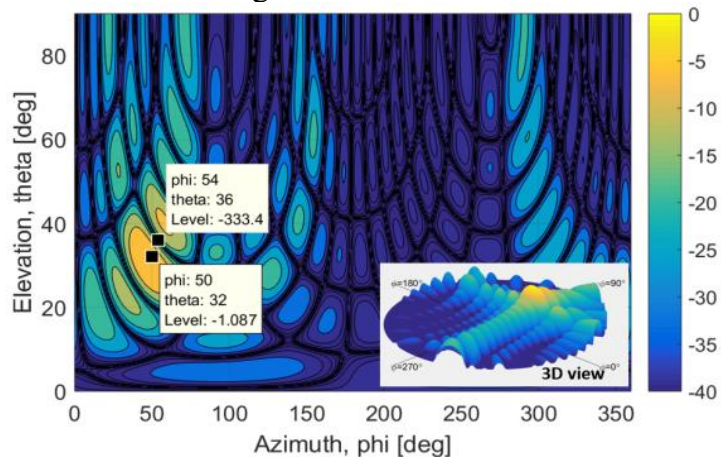


Fig. 6. Adaptive beamforming pattern using planar array with $8 \times 16 = 128$ elements, SOI: $\theta = 32^\circ$, $\varphi = 50^\circ$; SNOI: $\theta = 36^\circ$, $\varphi = 54^\circ$

The fourth simulation demonstrates the results of the case, which contains a higher antenna element number than a common development case, namely the planar array with $16 \times 16 = 256$ antenna elements (fig. 7). The beam maximum is directed toward the SOI UE with the radiation level $-1,076$ dB and one can see in the diagram that the SOI UE is now inside of the bright yellow ring. The null is placed exactly on the SNOI UE spot with its radiation field strength $-335,7$ dB. This simulation case has no big difference in compare to the previous one with 128 antenna elements.

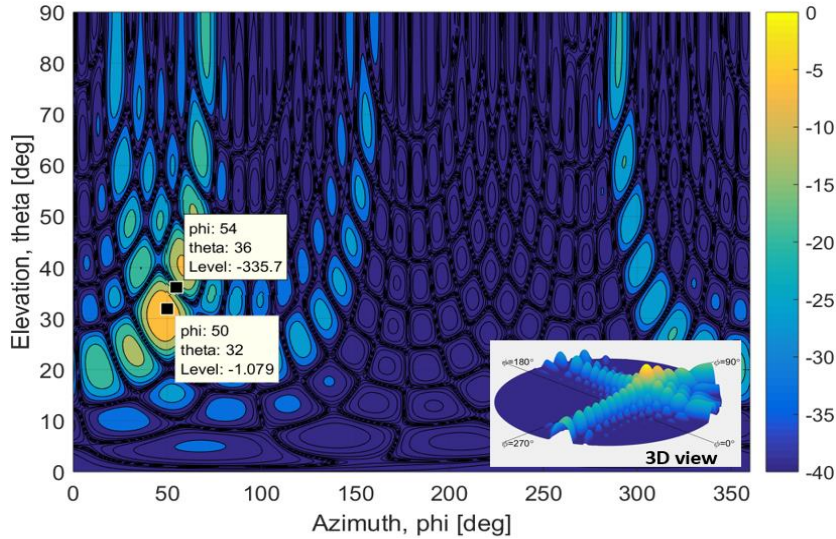


Fig. 7. Adaptive beamforming pattern using planar array with $16 \times 16 = 256$ elements, SOI: $\theta = 32^\circ$, $\varphi = 50^\circ$; SNOI: $\theta = 36^\circ$, $\varphi = 54^\circ$

The results of the last simulation case with large number of $32 \times 32 = 1024$ of antenna elements are showed in the fig. 8. The beam is directed exactly to the SOI UE, since the radiation level reaches here its highest value, as one can recognize in the diagram. At the same time the beam achieves here the narrowest form. In conduction with the highest field strength among all simulation cases it means, that this configuration provides the highest resolution of the beamforming. Moreover, the null steering has in this case the highest suppression of the antenna radiation in comparison to other simulation cases.

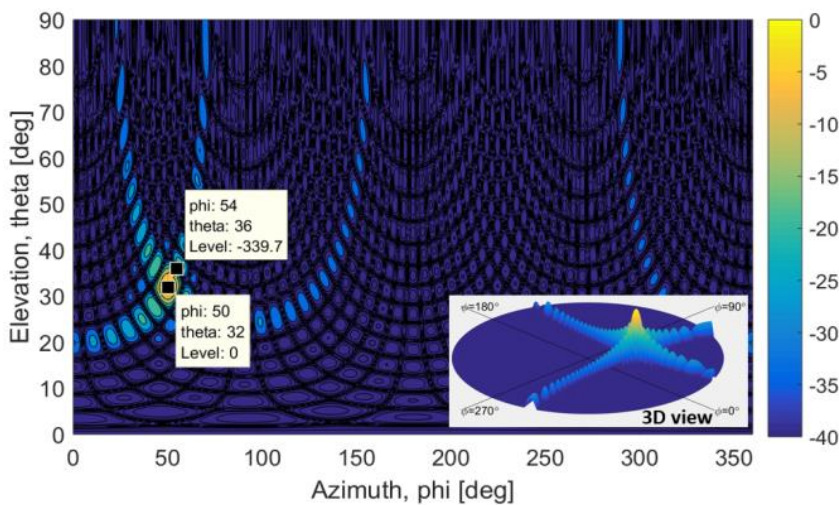


Fig. 8. Adaptive beamforming pattern using planar array with $32 \times 32 = 1024$ elements, SOI: $\theta = 32^\circ$, $\varphi = 50^\circ$; SNOI: $\theta = 36^\circ$, $\varphi = 54^\circ$

Another interesting fact can be seen here, that with a such large number of antenna elements the side lobes of the beamforming diagram practically absent. The summary of simulation results is presented in table 1.

Table 1. Simulation results summary

Array configuration, number of elements	SNOI suppression, dB	5G requirements fulfillment for moving UE 0,5 m/s
16	6	no
64	128	partially
128	332	yes
256	334	yes
1024	339,7	yes

It is well known, that angular resolution is tightly coupled with distance between gNB and UE, that's why to reveal practical recommendations for beamforming techniques deployment in 5G wireless communication systems and networks, let's now check 4° resolution capabilities for SOI and SNOI terrestrial separation in various cell types.

In the 3GPP specification [2] the following cell types are defined: indoor, dense urban, urban macro and rural, with the corresponding cell radius in 20 m, 200 m, 500 m and 5000 m. According to this definition we calculated and plotted possible distance between SOI and SNOI, which can be provided when the beamforming accuracy 4° is sustained (fig. 9): spatial separation of UEs is possible: for indoor cells up to 1,3 m; for dense urban cells up to 13,9 m; for macro urban cells up to 34,9 m; and for rural up to 350 m.

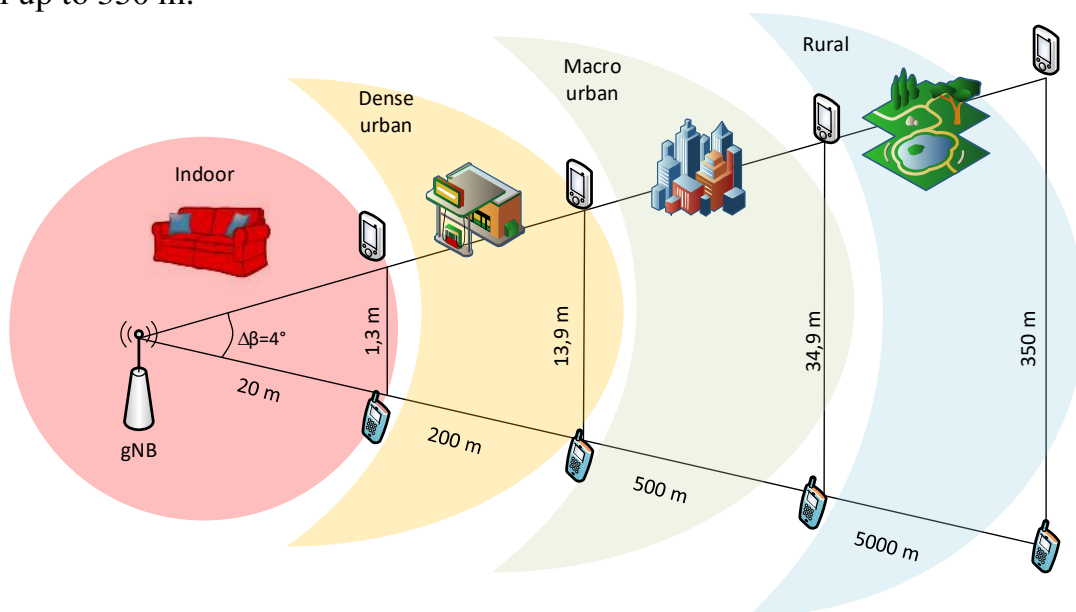


Fig. 9. Spatial separation of SOI and SNOI illustration for 3GPP cell types

4 Conclusion

Different planar array configurations, recommended by 3GPP [13] for 5G wireless communication systems and networks, were investigated in their resolution capabilities of beamforming and the null steering. LMS adaptive beamforming algorithm for planar antenna array configurations with 16, 64, 128, 256 and 1024 antenna elements was realized via simulation model so that to investigate its angular resolution bounds. Taking 3GPP requirement of 5° angular resolution for users moving up to 0,5 m/s into account, the accuracy 4° with 1° margin was investigated in this work for different planar arrays configurations.

Results of the current simulation research revealed that with the growth of the antenna elements from 128 not only the accuracy of the beamforming increases up to 4° angular resolution, but also null steering becomes precise, which provides interference suppression up to 340 dB and accordingly meets 5G requirements with margin.

Although 16 and 64 planar antenna elements configuration does not meet 3GPP accuracy requirements, it can cover another 5G goals, such as relaxed accuracy requirements of beamforming for pedestrian and static use cases, or capacity growth [23].

As for practical recommendations for beamforming techniques deployment in 5G wireless communication systems and networks, possible distance between SOI and SNOI, which can be provided when the beamforming accuracy 4° is sustained, is following: for indoor cells up to 1,3 m; for dense urban cells up to 13,9 m; for macro urban cells up to 34,9 m; and for rural up to 350 m.

Acknowledgements. The reported study was supported by the Ministry of Science and Education of the Russian Federation with Grant of the President of the Russian Federation for the state support of young Russian scientists № MK-3468.2018.9.

References

1. 3GPP TS 22.261 V16.5.0. Technical Specification Group Services and System Aspects; Stage 1; Service requirements for the 5G system; (Release 16). Sept. (2018).
2. 3GPP TR 38.913 V. 0.3. P 36. Study on Scenarios and Requirements for Next Generation Access Technologies (2016).
3. Constantine A.B. Antenna theory: analysis and design. Fourth edition, Wiley. 2016.
4. Stepanets I., Fokin G.: Features Of Massive MIMO In 5G networks. Last Mile, Nr.1, pp. 44-50. (2018).
5. Lo Y. T., Lee S. W. (Eds): Antenna Handbook, Theory, Applications, and Design, Chapter 11, pp. 49–52, Van Nostrand Reinhold Company, New York. (1988).
6. Giordani M, Polese M, Roy A, Castor D, Zorzi M. A.: Tutorial on Beam Management for 3GPP NR at mmWave Frequencies. arXiv preprint arXiv:1804.01908. Apr 5. (2018).
7. Fokin G.A.: Management of self-organizing packet radio networks based on radio stations with directional antennas, PhD thesis, The State University of Telecommunication St. Petersburg. (2009).

8. Godara LC.: Application of antenna arrays to mobile communications. II. Beam-forming and direction-of-arrival considerations. *Proceedings of the IEEE*. Aug; 85(8). (1997).
9. Q. Zou, Z. L. Yu, Z. Lin: A robust algorithm for linearly constrained adaptive beamforming. *IEEE Signal Processing Letters*, vol. 11, pp. 26-29, Jan. 2004.
10. Butler J., Lowe R.: Beam-Forming Matrix Simplifies Design of Electronically Scanned Antennas. *Electronic Design*, pp. 170-173, April 12. (1961).
11. Blass J.: Multidirectional Antenna: A New Approach to Stacked Beams, *IRE International Conference Record*, Vol. 8, Part 1. (1960).
12. S. Mano, et al.: Application of Planar Multibeam array Antennas to Diversity Reception, *Electronics and Communications in Japan*, Part 1, Vol. 79, No. 11, pp. 104-112. (1996).
13. Dietrich Jr, C. B.: Adaptive arrays and diversity antenna configurations for handheld wireless communication terminals (Doctoral dissertation, Virginia Tech). (2000).
14. Bakulin MG, Varukina LA, Kreindelin VB. *MIMO technology: principles and algorithms*. Moscow: Goryachaya Liniya–Telekom. (2014).
15. Khoshnevis B, Yu W, Adve R.: Grassmannian beamforming for MIMO amplify-and-forward relaying. *IEEE Journal on Selected Areas in Communications*. Oct. 26. (2008).
16. Maskulainen I, Luoto P, Pirinen P, Bennis M, Horneman K, Latva-aho M.: Performance evaluation of adaptive beamforming in 5G-V2X networks. In *Networks and Communications (EuCNC), IEEE European Conference on 2017 Jun 12*. pp. 1-5. (2017)
17. Andersson S., Tidelund W.: *Adaptive Beamforming for Next Generation Cellular System*. (2016).
18. Chen, Shanzhi, Shaohui Sun, Qiubin Gao, Xin Su: Adaptive beamforming in TDD-based mobile communication systems: State of the art and 5G research directions. *IEEE Wireless Communications* 23, no. 6 pp. 81-87 (2016).
19. Khalaf, Ashraf AM, Abdel-Rahman BM El-Daly, Hesham FA Hamed: Different adaptive beamforming algorithms for performance investigation of smart antenna system. *Software, Telecommunications and Computer Networks (SoftCOM), 2016 24th International Conference on*, pp. 1-6. IEEE (2016).
20. Surendra, L., Shameem, S. and Khan, D.H.: Performance comparison of LMS, SMI and RLS adaptive beamforming algorithms for smart antennas. *International Journal Of Computer Science And Technology (IJCST)*, 3, pp.973-977 (2012).
21. 3GPP, “Framework for beamformed access”, Samsung - Tdoc R1- 164013 (2016).
22. 3GPP, “Analog/digital/hybrid beamforming for massive MIMO”, Samsung, RAN1#85, R1-164018, May (2016).
23. Stepanets I, Fokin G., Müller A.: Capacity estimation ways of massive MIMO systems. *T-Comm Telecommunication and transport*, vol. 10 (2018).